Organic & Biomolecular Chemistry

PAPER

View Article Online
View Journal | View Issue





Cite this: *Org. Biomol. Chem.*, 2018, **16**, 8115

# Syntheses and anti-cancer activity of CO-releasing molecules with targeting galactose receptors†

Jili Li,[a] Jinlong Zhang,[a] Qiuping Zhang,[a] Zhongjie Bai,[a] Quanyi Zhao,*[a] Dian He,*[a] Zhen Wang,[a] Yonglin Chen[b] and Bin Liu[c]

CO-releasing molecules (CORMs) containing cobalt have many bioactivities, but most of them do not dissolve in water and have no selectivity to tissue and organs. On the basis of the specific recognition of galactose or sialic acid by a receptor, a series of CORMs based on carbohydrates were synthesized and evaluated. The test results show that all the complexes displayed anticancer activity. Among them, the effects of the complexes of galactose (**1**), GalNAc (**8**) and sialic acid (**10**) were very distinct. Complex **1** displayed higher activity against HeLa, HePG2, MCF-7 and HT-29 cell proliferation than *cis*-platin (DDP), and its selectivity was far much better than DDP compared with normal cell W138. Furthermore, the uptakes of complexes **1**, **8** and **10** by HePG2, HT-29, A549 and RAW264.7 cell lines were studied. The uptake ratio of each cell line for complex **1** was different, and the order of uptake ratio in the four cell lines was HePG2 > HT-29 > RAW264.7 > A549. The HePG2 cells absorbed complex **1** beyond 60% after incubation for 8 h, while A549 absorbed only 27.8%. For complex **8**, the uptake trend was similar to that of complex **1** with it being absorbed by all the four cancer cells, but the uptake rate was lower. However, differently, complex **10** was absorbed heavily by macrophage RAW264.7, followed by HePG2; after 8 h incubation, the uptake ratio of RAW264.7 was over 50%. In addition, the mechanism of action was explored, and the results showed that the complexes inhibited cell cycle arrest at the G2/M phase; complex **1** up-regulated the expression levels of caspase-3 and Bax, and down-regulated the Bcl-2 expression, giving rise to HePG2 cell apoptosis.

Received 7th August 2018,
Accepted 9th October 2018

DOI: 10.1039/c8ob01921e

rsc.li/obc

## 1. Introduction

CO has potential in clinics because it is involved in neurodegeneration,[1] hypertension,[2] inflammation,[3–5] oxidative stress,[6,7] cell proliferation,[8] and apoptosis.[9,10] However, the application of CO gas in the clinic remains questionable due to its toxicity and lack of quantitative control.[11] For this reason, Motterlini proposed the concept of CO releasing molecules (CORMs) ten years ago.[12] Over the next few years, a number of CORMs containing Ru, Fe, Mn, Co, and Mo were synthesized. The test results showed that most of them exhibited cytoprotective, anti-inflammatory, vasodilatory and other beneficial effects.[13–15]

Among these CORMs, the complexes based on cobalt were paid more attention than others.[16] The complex containing a $[Co_2(CO)_6]$ moiety has been studied widely as an antitumor reagent. Hexacarbonyl-[2-propinyl acetylsalicylate] dicobalt displayed higher activity against MCF-7 and MDA-MB-231 than *cis*-platin,[17] and its analogue was effective against hormone dependent tumors.[18] In addition to anti-cancer activity, these complexes also displayed anti-inflammatory activity. The researchers found that their anti-inflammatory effects were due to liberating CO to inhibit nitrite,[19] and the effects of proliferative inhibition of cancer cells were mainly resulting from the CO to inhibit Hsp90 downstream protein activity, such as Akt, ER alpha, and cyclin D1.[20] In addition, the complexes also promoted apoptosis, disturbed cell cycle and interfered with DNA synthesis.[21]

Though Co-CORMs have good biological activity, they are almost insoluble in water and have no selectivity to tissue and organs. Recently, T. Tsubomura *et al.* found that carbohydrate complexes of palladium and platinum had antitumor activity *in vitro* and *in vivo*;[22–26] in 2004, D. Schlawe found that iron-carbonyl complexes had cytotoxicity and triggered apoptotic effects.[27] After that, the CORMs modified with fructose were found to induce apoptosis at high millimolar concentrations;[28] and three new derivatives displayed activity against MCF-7 cells.[29,30]

[a]*Institute of Medicinal Chemistry, School of Pharmacy of Lanzhou University, Lanzhou 730000, China. E-mail: zhaoqy@lzu.edu.cn, hed@lzu.edu.cn; Fax: +869318915686; Tel: +869318915686*
[b]*The First Affiliated Hospital of Lanzhou University, Lanzhou 730000, China*
[c]*School of Stomatology of Lanzhou University, Lanzhou 730000, China*
†Electronic supplementary information (ESI) available. See DOI: 10.1039/c8ob01921e

Generally, galactose is specifically recognized and bound by galectin and the asialoglycoprotein receptor (ASGP-R). Galactose lectin is closely related to the development of tumors. The over-expression of galectin-3 in colon cancer cells was involved in the process of carcinogenesis, development and metastasis of colon cancer. ASGP-R is a transmembrane protein of the membrane surface of hepatocytes; when the molecules containing the galactose residue bind to the ASGP-R, it can be transported to lysosomes. The sialic acid receptor is siglec-1, which has high expression on (tam) tumor-associated macrophages. Siglec is an endocytosis receptor that transports drugs into target cells. Sialic acid (SA) and its derivatives may be used as carriers for drug transport, which can transport anticancer drugs to tumor-associated macrophages, and inhibit tumor growth and metastasis.

Therefore, we have synthesized a series of CORMs with carbohydrates including galactose and sialic acid, and found that they not only have good solubility in water, but also target organs or tumor-associated macrophages to give rise to anti-tumor activity.

## 2. Results and discussion

### 2.1. Syntheses and characterization

All complexes **1–7** were synthesized using sugar as the starting material. Sugar mainly included galactose, methyl glucuronate, mannose, *etc*. Complexes **1–7** were prepared by the reaction of carbohydrates $\mathbf{A_{1-7}}$ and acetic anhydride to form acetylated sugars, and then reacted with thiourea in the presence of boron trifluoride to form active intermediates, which reacted with propargyl bromide to afford $\mathbf{B_{1-7}}$;[31–34] $\mathbf{B_{1-7}}$ was deacetylated using sodium methoxide to afford the deacetylated products, and then reacted with octacarbonyl dichromate to obtain the target molecules **1–7**. For complexes **8–9**, the starting material was amino sugar; the intermediates $\mathbf{B_{8-9}}$ were obtained in the presence of ytterbium trifluorosulfonate.[35,36] Sialic acid was treated by the reaction of esterification, then acetylation, glycosylation and deacetylation, and finally reacted with cobalt carbonyl to afford complex **10**.[37,38]

The complexes were either a red-black oil or red solid, and stable in air for several days. They are soluble in water, and easily soluble in polar organic solvents, including $CH_3OH$, DMF and DMSO. Complexes **Ac-1–10** easily dissolve in organic solvents, but do not dissolve in water. All the complexes showed a number of strong terminal carbonyl absorption bands at 2079–1849 $cm^{-1}$ in their IR spectra. The higher absorption bands were attributed to terminal carbonyls coordinated to the Co atom. The IR spectra showed the corresponding ester carbonyl absorptions at 1755–1735 $cm^{-1}$ for complexes Ac-**1–9**; for the spectra of complexes **8**, **Ac-8**, **9** and **Ac-9**, there was another strong carbonyl absorption band of the acetamido group at 1680–1700 $cm^{-1}$. Because of the paramagnetism of cobalt atoms, the peaks in the $^1H$ NMR spectra became wider, and some characteristic signals were superimposed. In the $^1H$ NMR spectra of complexes **1–10**, the chemical shifts of the protons on the carbon connected with two cobalt atoms were observed at 6.08–5.98 ppm as a singlet; and the chemical shifts of protons on the carbon of the carbohydrate were observed at 4.79–5.29 ppm. In the $^{13}C$ NMR spectra of the complexes **1–10**, the signals at about 90 ppm were assigned to $C_1$ of the carbohydrates.

Introducing carbohydrates into CORMs increased their solubility in water. The lg*P* values of complexes **1–10** were in the range of 1.16 and 1.32, which indicated that their polarity increased greatly. The lg*P* values of complexes **Ac-1–10** were between 1.86 and 2.28 (Table 1), and distinctly, they have lower polarity than the corresponding unacylated complexes. Compared with the previously reported complexes,[39,40] the carbohydrate structures in the complexes not only help them to dissolve in water, but also decrease metal cobalt toxicity (Schemes 1–3).

### 2.2. CO-releasing tests

Deoxymyoglobin (deoxy-Mb) has a high affinity for CO, binding one CO to form carbonyl myoglobin (CO-Mb). The difference between the absorption maxima of deoxy-Mb and CO-Mb allows the detection of CO-release from CORMs. The maximal absorption peak of deoxy-Mb appears at 560 nm while the two maximal absorption peaks of Mb-CO appear at 540 and 578 nm.

The CO-release ability was therefore evaluated in a myoglobin-based aqueous assay. A solution of deoxy-Mb was prepared and subsequently treated with an aqueous solution of CORMs at 37.5 °C. The resulting conversion of deoxy-Mb to CO-Mb was monitored by UV-Vis spectroscopy. To evaluate both the total amount of CO released and the rate of CO-release, all complexes were tested at 40 μM concentration by following the changes in absorption. The UV spectra of some complexes and the concentrations of CO-Mb as a function of time are given in Fig. 1. The half-lives of some complexes are listed in Table 1. As seen from the data, all complexes **1–10** were effective releasers with half-lives varying between 30.6 min and 48.1 min, and most of them were about 40 min. They are slower CO releasers, and their half-lives ($t_{1/2}$) are longer than CORMs containing ruthenium.[41] After acylation of the complexes, acylated complexes released CO faster than the corresponding com-

**Table 1** Physical–chemicalparameters of all the complexes

| Complex | $T_{1/2}$ (min) | lg*P* | Complex | $T_{1/2}$ (min) | lg *P* |
|---|---|---|---|---|---|
| **1** | 42.8 | 1.16 | **6** | 40.6 | 1.23 |
| **Ac-1** | 44.1 | 1.86 | **Ac-6** | 33.8 | 2.06 |
| **2** | 47.9 | 1.19 | **7** | 30.6 | 1.25 |
| **Ac-2** | 49.6 | 1.92 | **Ac-7** | 34.9 | 2.12 |
| **3** | 32.6 | 1.23 | **8** | 38.6 | 1.26 |
| **Ac-3** | 36.8 | 2.10 | **Ac-8** | 42.6 | 1.98 |
| **4** | 44.2 | 1.21 | **9** | 39.6 | 1.22 |
| **Ac-4** | 46.4 | 1.82 | **Ac-9** | 44.8 | 2.08 |
| **5** | 48.1 | 1.20 | **10** | 38.2 | 1.32 |
| **Ac-5** | 46.2 | 1.98 | **Ac-10** | 40.6 | 2.28 |

**Ac** appoints the acetylated product of the complex.

 

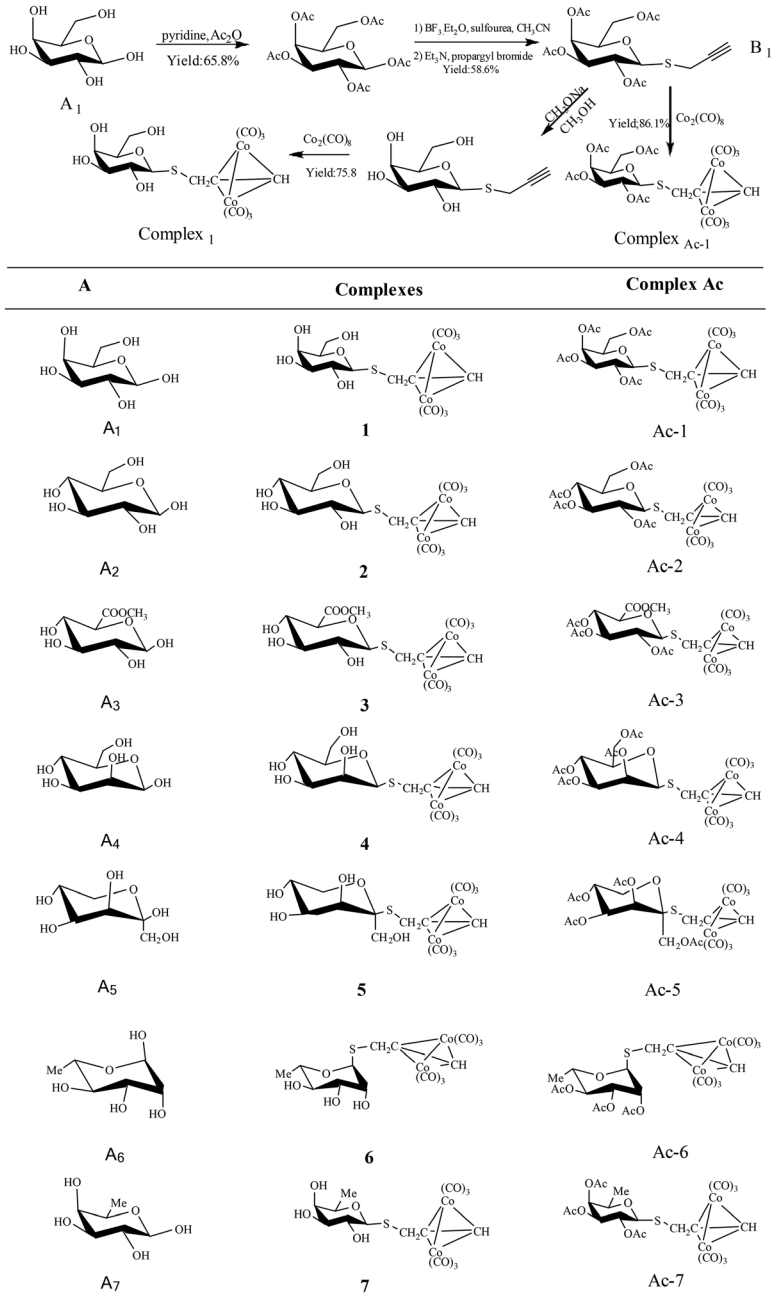


**Scheme 1** Syntheses and structures of complexes **1–7**.

plexes except for complexes **5** and **6**. This is possibly because acylation of the hydroxyls in complexes **1–10** decreased disturb of the hydroxyl group to CO releasing. In addition, the half-lives of CO release were connected with the structures of the carbohydrate.

**2.2.3 Anti-tumor activities of the complexes.** In order to obtain more information about anticancer activity, we chose HeLa, A549, HePG2, MCF-7 and HT-29 as test cancer lines; all the complexes were evaluated for the growth inhibitory effect by the MTT method. Cis-platin (DDP) was used as a positive control in the process of testing. As shown in Table 2, all the complexes displayed cell proliferative inhibition activities to some degree, and their $IC_{50}$ values were in the 5.69–149.02 μM range. All complexes **1–10** displayed higher activities than their corresponding acetylated products. Among complexes **1–10**, complexes **1**, **8** and **10** displayed higher activities than the others. Complex **1** displayed higher activities against HeLa, HePG2, MCF-7 and HT-29 cell proliferation than DDP. Its efficacy ($IC_{50}$ 5.69 μM) was about as high as 2.8 times DDP (15.87 μM) against HePG2 cell proliferation, and 2.3 times (21.96 μM) against HT-29 cells. Meanwhile, complex **1** displayed better activity against MCF-7 cell proliferation than

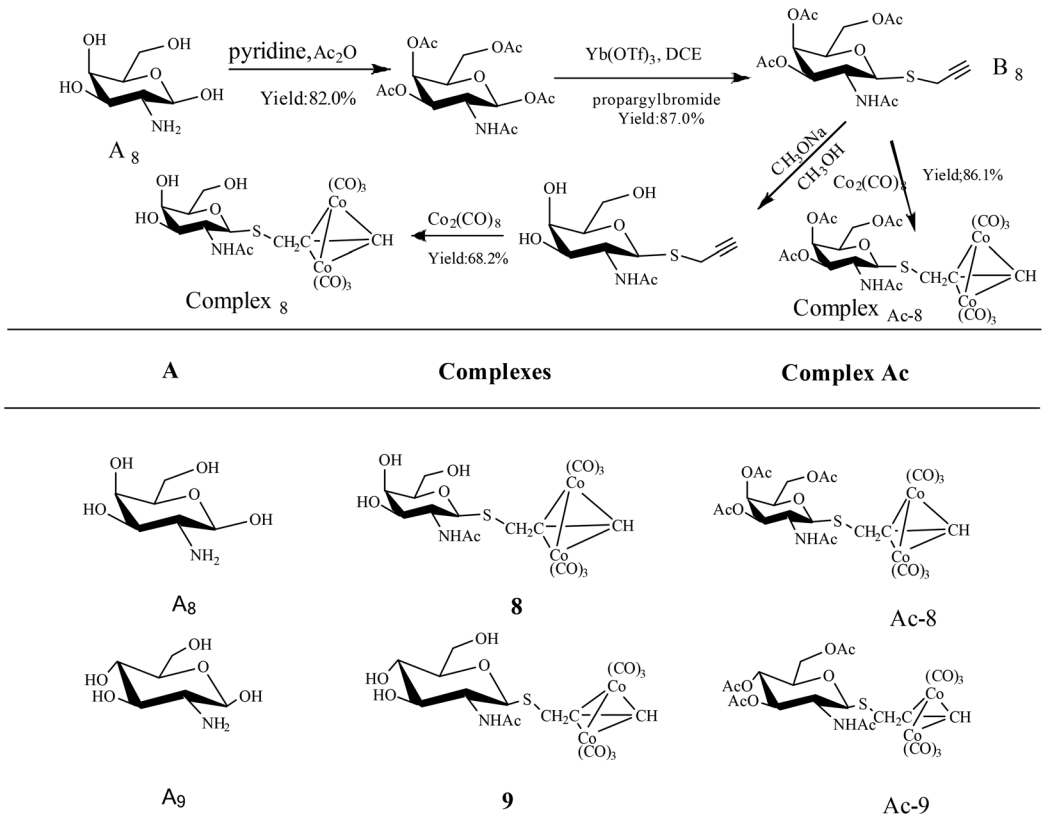


**Scheme 2** Syntheses and structures of complexes **8–9**.

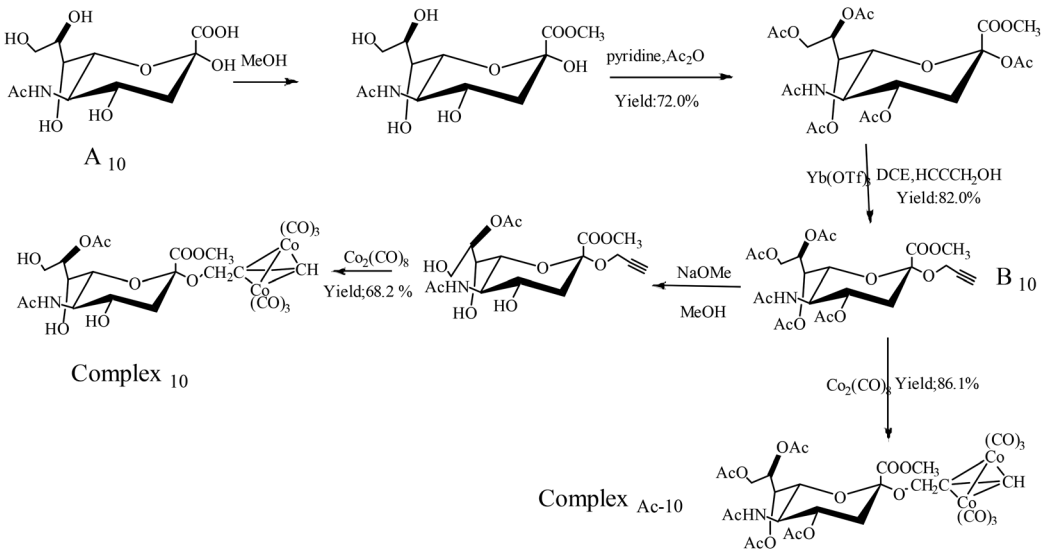


**Scheme 3** Synthesis and structure of complex **10**.

DDP. For normal cell W138, the selectivity of complex **1** was far better than that of DDP. Complex **8** had a similar inhibitory effect to complex **1** for all the cancer cells, and its efficacy was lower than that of complex **1** for all the cell lines but HeLa cells. This demonstrates that the structure of the complex was connected with its effect. In all, complexes **1** and **8** had good activity against the proliferation of HePG2 cell lines. This may be related to the over-expression of the galactose receptor on the surface of HePG2 cells. Complex **10** displayed the highest activity against A549 cells among the tested cell lines, and its $IC_{50}$ value was 9.74 μM. It suggests that complex **10** has selectivity to A549 cells to some degree.

 

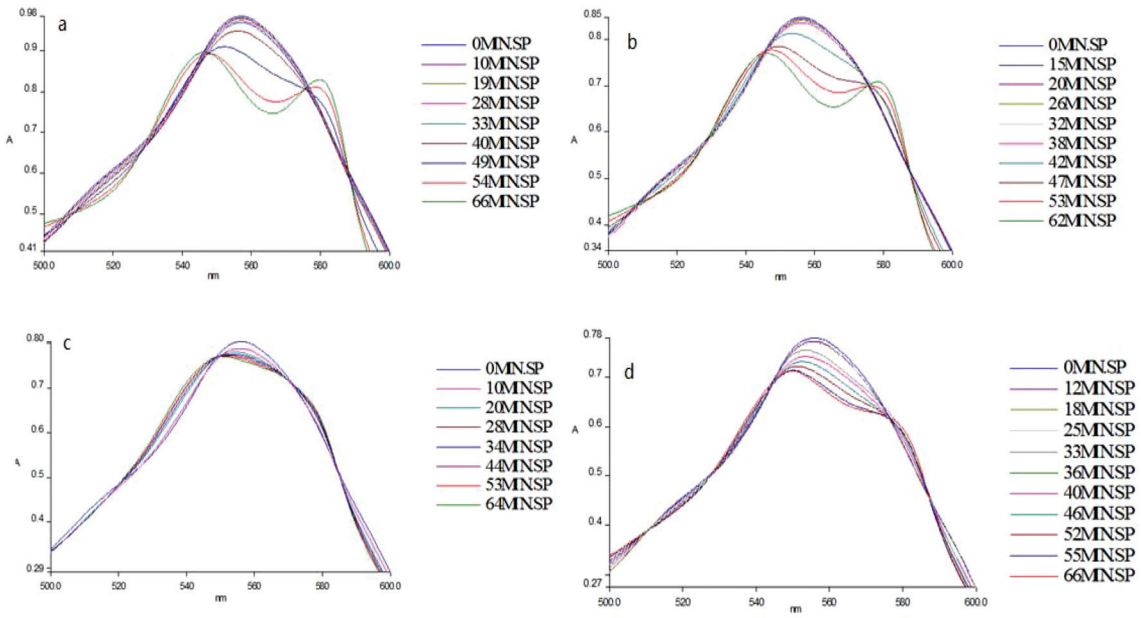


**Fig. 1** The typical changes in the electronic spectrum of myoglobin as CO releasing from compounds (myoglobin binds one CO to form carbonyl myoglobin), a, complex **1** (10 μM); b for **2** (10 μM); c for **8** (10 μM); d for **10** (10 μM).

**Table 2** $IC_{50}$ values of complexes to the tumor cells and W138[a]

| | $IC_{50}$ (μM) | | | | | |
|---|---|---|---|---|---|---|
| Complex | HeLa | A549 | HePG2 | MCF-7 | HT-29 | W138 |
| **1** | 16.26 ± 0.18 | 14.17 ± 0.14 | 5.69 ± 0.21 | 14.92 ± 0.17 | 9.62 ± 0.15 | 36.74 ± 0.22 |
| **Ac-1** | 19.82 ± 0.22 | 21.16 ± 0.34 | 26.63 ± 0.33 | 32.27 ± 0.29 | 20.54 ± 0.32 | 30.75 ± 0.28 |
| **2** | 20.52 ± 0.12 | 17.09 ± 0.22 | 16.82 ± 0.32 | 14.53 ± 0.42 | 21.16 ± 0.29 | 24.68 ± 0.27 |
| **Ac-2** | 35.21 ± 0.16 | 29.46 ± 0.41 | 24.52 ± 0.33 | 20.17 ± 0.36 | 27.46 ± 0.44 | 35.25 ± 0.29 |
| **3** | 42.84 ± 0.27 | 29.68 ± 0.18 | 34.52 ± 0.31 | 62.35 ± 0.37 | 58.27 ± 0.42 | 69.27 ± 0.30 |
| **Ac-3** | 52.73 ± 0.31 | 62.51 ± 0.41 | 70.24 ± 0.42 | 48.92 ± 0.38 | 67.62 ± 0.51 | 78.79 ± 0.26 |
| **4** | 82.49 ± 0.29 | 78.67 ± 0.31 | 58.63 ± 0.19 | 64.29 ± 0.27 | 59.81 ± 0.33 | 80.56 ± 0.21 |
| **Ac-4** | 119.74 ± 0.19 | 101.23 ± 0.5 | 113.81 ± 0.6 | 92.41 ± 0.48 | 139.02 ± 0.6 | 129.67 ± 0.4 |
| **5** | 56.73 ± 0.21 | 49.63 ± 0.32 | 67.47 ± 0.37 | 71.28 ± 0.28 | 69.46 ± 0.30 | 77.34 ± 0.41 |
| **Ac-5** | 149.02 ± 0.26 | 110.81 ± 0.4 | 118.06 ± 0.5 | 128.54 ± 0.6 | 131.27 ± 0.6 | 145.87 ± 0.7 |
| **6** | 28.43 ± 0.23 | 42.51 ± 0.26 | 36.24 ± 0.29 | 37.68 ± 0.20 | 24.78 ± 0.28 | 55.36 ± 0.19 |
| **Ac-6** | 90.03 ± 0.29 | 126.75 ± 0.6 | 89.28 ± 0.33 | 111.54 ± 0.3 | 118.26 ± 0.4 | 131.36 ± 0.5 |
| **7** | 54.74 ± 0.11 | 74.07 ± 0.41 | 49.35 ± 0.23 | 62.13 ± 0.19 | 56.32 ± 0.31 | 80.08 ± 0.29 |
| **Ac-7** | 117.34 ± 0.36 | 128.65 ± 0.6 | 85.23 ± 0.45 | 94.87 ± 0.39 | 90.85 ± 0.41 | 123.58 ± 0.4 |
| **8** | 13.84 ± 0.16 | 14.43 ± 0.14 | 7.69 ± 0.19 | 16.41 ± 0.22 | 12.36 ± 0.24 | 19.56 ± 0.14 |
| **Ac-8** | 63.59 ± 0.29 | 56.49 ± 0.28 | 52.16 ± 0.32 | 71.52 ± 0.37 | 85.48 ± 0.41 | 88.91 ± 0.35 |
| **9** | 21.38 ± 0.19 | 18.74 ± 0.27 | 22.02 ± 0.41 | 26.32 ± 0.47 | 20.28 ± 0.25 | 28.94 ± 0.23 |
| **Ac-9** | 84.74 ± 0.33 | 76.25 ± 0.39 | 59.07 ± 0.45 | 57.68 ± 0.51 | 73.24 ± 0.49 | 85.38 ± 0.39 |
| **10** | 10.23 ± 0.20 | 9.74 ± 0.18 | 11.03 ± 0.15 | 11.32 ± 0.17 | 17.14 ± 0.21 | 20.15 ± 0.24 |
| **Ac-10** | 18.67 ± 0.33 | 26.73 ± 0.22 | 33.74 ± 0.27 | 22.36 ± 0.33 | 30.25 ± 0.41 | 38.19 ± 0.41 |
| **DDP** | 18.74 ± 0.28 | 13.63 ± 0.20 | 15.87 ± 0.19 | 18.24 ± 0.33 | 21.96 ± 0.17 | 22.19 ± 0.33 |

[a] Values represent mean ± SEM from at least three independent experiments.

**2.2.4 Cellular uptake of the complex.** In order to further demonstrate that some complexes had selective proliferation inhibitory activity toward cancer cells, the uptakes of complexes **1**, **8** and **10** by HePG2, HT-29, A549 and RAW264.7 cells were studied respectively. For this purpose, the cells were exposed to **1**, **8** or **10** over a period of 2 h, 4 h and 8 h, and then the metal levels of the cells were measured by using inductively coupled plasma mass spectrometry (ICP-MS, see the Experimental section for more details).[42–45] The results are shown in Fig. 2. We can see that the uptake of target molecules by three kinds of tumor cells and macrophage RAW264.7 gradually increased with the prolongation of time. The uptake of the same cell line to different complexes was different, and for the same complex, the uptake of different cell lines varies greatly.

For complex **1**, after 8 h of incubation, the uptake of every cell line was more distinct than the control, but HePG2 cells

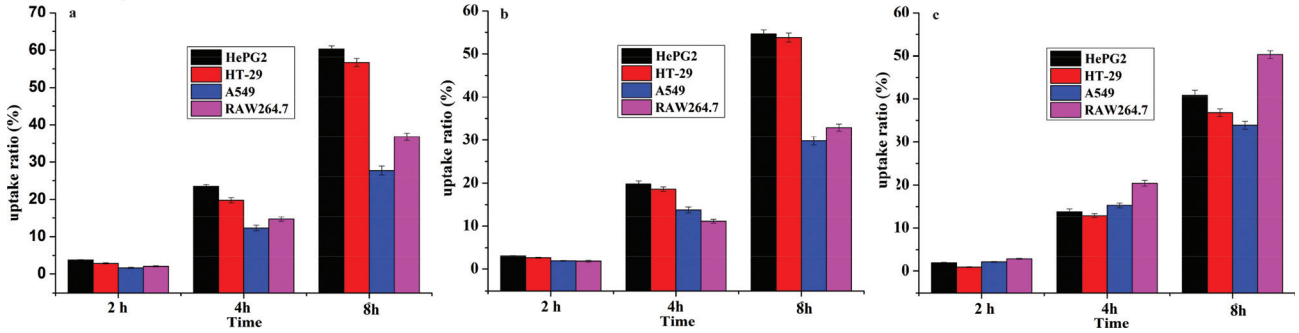


Fig. 2 The uptake of the complex with the time, (a) for complex **1**, (b) for **8** and (c) for **10**.

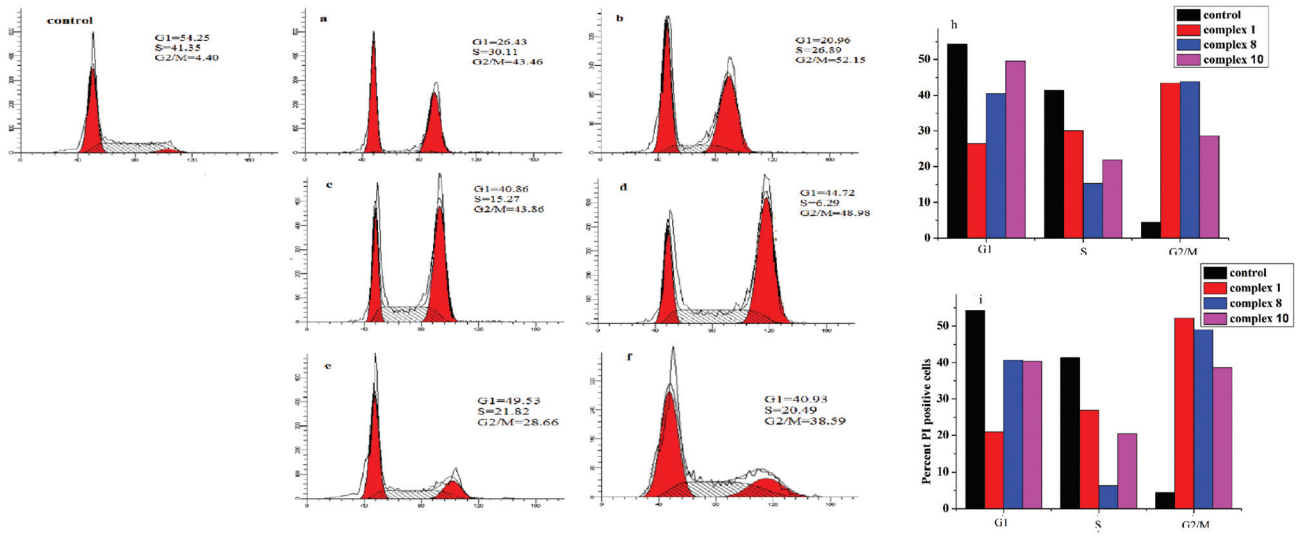


Fig. 3 Effects of the complexes on the HePG2 cell cycle: a and b are for complex **1** with 10 μM and 20 μM; c and d for complex **8**; e and f for complex **10**; h for treatment with 10 μM; i with 20 μM.

absorbed it far much more than the other cell lines. The uptake ratios for HePG2 for 2 h, 4 h and 8 h were about 3.7%, 23.5% and 60.3%, respectively. The uptake ratio of each cancer cell line was different, and the order of uptake ratio was HePG2 > HT-29 > RAW264.7 > A549. After 8 h, the uptake ratio of HePG2 was more than 60%, while that of A549 was only 27.8%. For complex **8**, the uptakes of the four cells were similar to those of complex **1**, but the uptake rates were lower than those of complex **1**. Unexpectedly, complex **10** was absorbed heavily by macrophage RAW264.7, followed by HePG2; and the uptake ratio of the other two kinds of cells was about as much as each other. After 8 h incubation, the uptake ratio of RAW264.7 for complex **10** was more than 50%.

The structure of the complex has a great influence on its bio-distribution and activity. Complexes **1** and **8** were ingested in large quantities by HePG2, this is because both of them contain galactose and amino-galactose structural units, which are recognized by the galactose receptor on the cell membrane of the HePG2 cells. Possibly, it was through the receptor selective recognition that the complexes aggregated to the surface of the cancer cell, and entered into the cell by endocytosis. However, under the same conditions, the uptake of complex **8** was less than that of complex **1** for every cell line. This suggests that the amino group takes the place of the hydroxyl group at the 2-position in galactose attenuating the binding ability to the galactose receptor. Complex **10** was absorbed heavily by macrophage RAW264.7, this is because complex **10** has a sialic acid unit, which is selectively recognized by the sialic acid receptor. Macrophages are connected with some immune diseases, so complex **10** possibly has a controlling effect on immune diseases.

**2.2.5 Effects of complex on cell cycle and apoptosis.** To investigate whether the complexes have anti-mitotic effects on HePG2 cells, cell cycle analysis was performed by flow cytometry. The treatment of HePG2 cells with 10 μM and 20 μM complexes for 24 h resulted in significant alterations in cell cycle phases. The results are shown in Fig. 3. For every tested complex, there was a significant increase in the percentage of the cells at the pre-G2/M phase with the increase in the concentration. When HePG2 cells were treated with complex **1** at

 

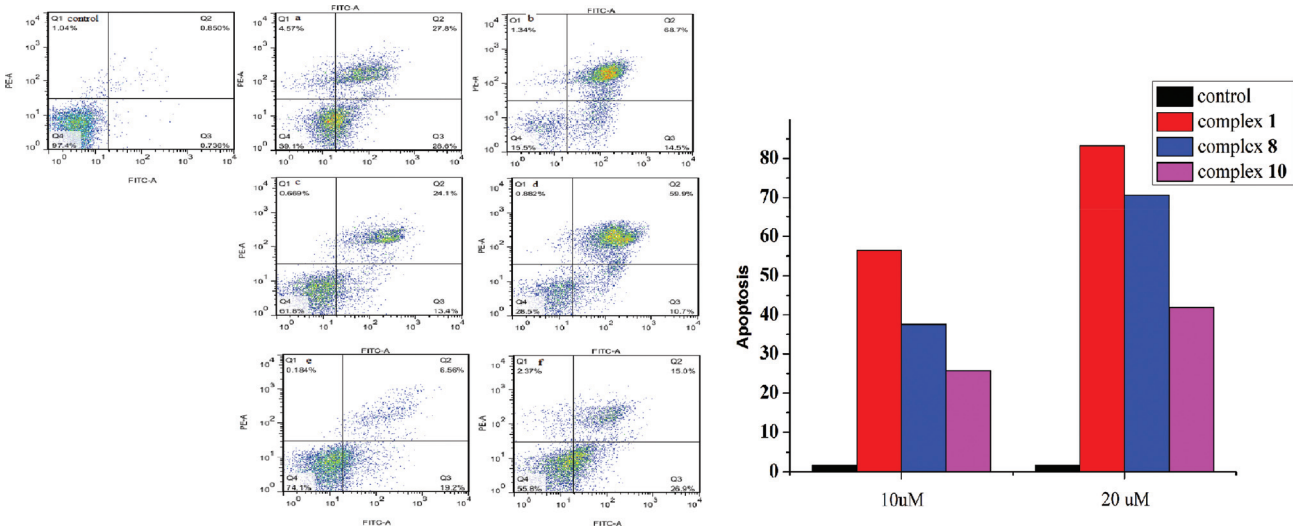


**Fig. 4** Effects of the complexes on HePG2 cell apoptosis: a and b are for complex **1** with 10 μM and 20 μM; c and d for complex **8**; e and f for complex **10**.

20 μM, the percentage accounted for 52.15%, while that of the control was 4.40%; under the same condition, it was 48.98% with complex **8** and 25.59% with complex **10**. Hence, we conclude that the complexes inhibited the cell proliferation through cell cycle arrest at the G2/M phase.

The complexes arrested the cell cycle at the G2/M phase, so they almost surely induce apoptosis in HePG2 cells. In order to obtain more information about apoptosis, we further performed apoptosis detection in a dose-dependent manner (Fig. 4). We first treated HePG2 cells with varying concentrations (10 and 20 μM) of the complexes. Then AnnexinV-FITC/PI assay was performed with the cells. As a result, HePG2 cells showed considerable sensitivity to the tested complexes, and their effects were in a dose-dependent manner. When the complexes were 20 μM, the proportion of apoptotic cells was up to 83.20% for complex **1**; under the same conditions, it was 70.6% for complex **8** and 41.9% for complex **10**. Thus, it can be concluded that the complexes significantly induced apoptosis of HePG2 cells in a dose dependent manner.

**2.2.6 Mechanism of action of the complex.** How did the complexes work? In order to understand more intuitively the effect of complexes on organelles, we made a morphological observation through fluorescence staining. After treating with the control or the complexes for 24 h, the HePG2 cells were washed with phosphate buffered saline (PBS) and immobilized with 3.7% paraformaldehyde PBS solution at room temperature for 10 min. The immobilized cells were washed with PBS and stained with 4′,6-diamidino-2-phenylindole (DAPI) and Mito-Tracker Green for 20 minutes at room temperature. Then, the cells were washed with PBS and observed using a fluorescence microscope.

Under the fluorescence microscope, the fluorescence of the cells in the control group was more diffuse and uniform, the nucleus was relatively complete and regular, the nucleus was ellipsoid, and the nucleolus was obvious (Fig. 5a). The mitochondria were short rod or ball shaped, and the shape was

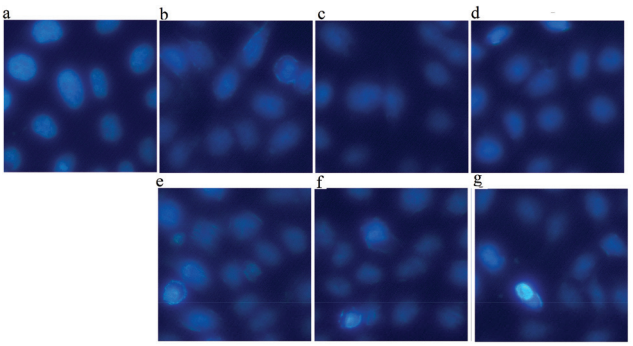


**Fig. 5** The nucleus of HePG2 cells by DAPI and Mito-Tracker Green fluorescence staining: a (control), b, c, d are for complex **1**, complex **8** and complex **10** with 10 μM; e, f, g are for complex **1**, complex **8** and complex **10** with 20 μM.

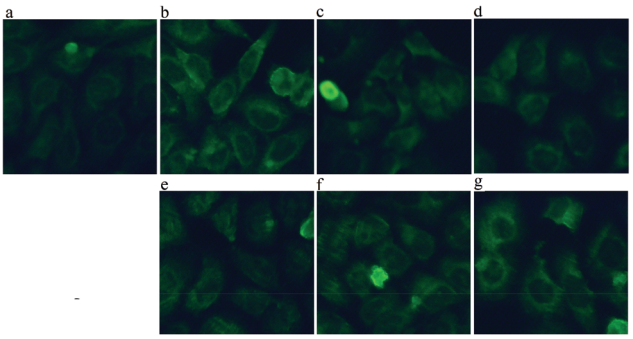


**Fig. 6** The mitochondria of HePG2 cells by DAPI and Mito-Tracker Green fluorescence staining: a (control), b, c, and d are for complex **1**, complex **8** and complex **10** with 10 μM; e, f and g are for complex **1**, complex **8** and complex **10** with 20 μM.

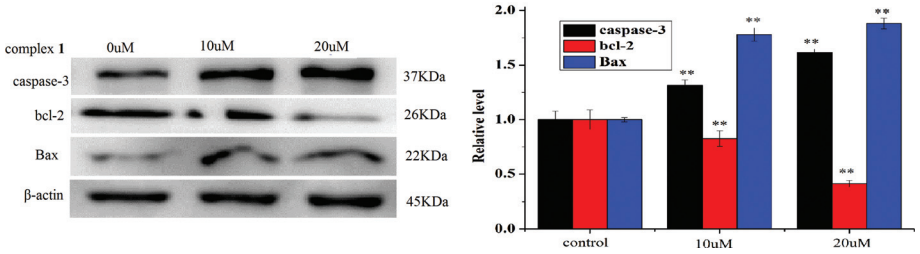


**Fig. 7** Effects of complex **1** on the protein levels in human HePG2 cells. HePG2 cells were exposed to 10 or 20 μM complex **1** for 24 h. The cell extract protein isolated from complex **1** treated HePG2 cells was subjected to Tris-glycine gel electrophoresis and immunoblotted with the antibodies against caspase-3, Bcl-2 or Bax. β-Actin was used as a loading control. Western blot data presented are representative of those obtained from three separate experiments.

regular. The central depression was the location of the nucleus, and it was obvious (Fig. 6a). But when the cells were exposed to the test complex for some time, the cell nucleus and mitochondria were obviously damaged. Most nuclei were densified or edge-stained, or densified in mass; some nucleoli disappeared and nucleolysis occurred in some nuclei (Fig. 5b–g). Mitochondria showed pyknosis, smaller matrices, deeper matrices, irregular morphology, less obvious nucleus position, and an increased number of apoptotic cells. When the concentration of the complex was 10 μM, the damage to the nucleus and mitochondria was slight; but when the concentration of the complex was 20 μM, the damage degree of the nucleus and mitochondria became more serious.

To further elucidate the mechanism of apoptosis induced by the complexes, the expression levels of three apoptosis-regulating genes in the bcl-2 protein family and caspase family were measured. Among them, the *bcl-2* gene and *bax* gene are two important regulatory genes which have opposite functions in the process of apoptosis regulation. *Bcl-2* inhibits apoptosis, while *bax* promotes apoptosis. Caspase-3 is a key protease in the process of apoptosis. The results showed that, compared with the control group, the expression of caspase-3 and Bax in the cells treated with the complex up-regulated obviously, but the Bcl-2 down-regulated (Fig. 7). When the complex concentration was 20 μM, the change in protein expression levels was obviously higher than that of the control group. The expression amount of caspase-3 (the death executive protein) was 2 times higher than that of the control; and bax (apoptosis-promoting protein) increased by 80% of the control, but the expression of bcl-2 (anti-apoptotic protein) decreased by about 40% of the control. This indicated that complex **1** induced HePG2 cell apoptosis by affecting the expression of the apoptotic gene.

## 3. Conclusion

CORMs containing cobalt have many bioactivities, such as anti-inflammatory and antitumor cell proliferation. The complexes displayed a lower toxicity in animal tests. Though the complexes damaged the liver and kidney after several consecutive administrations, the cobalt did not accumulate, and was excreted with the urine. In view of these aspects, the CORMs based on cobalt have potential to be a medicine. The structure-activity relationship study suggests that the complex biodistribution is related to side chain substituents, and the alkyne substituents significantly affect the rate of CO-release, cytotoxicity and cell viability. However, it is a pity that, at present, most CORMs obtained have a poor solubility and no selectivity to tissue and organs.

For this purpose, a series of CORMs based on carbohydrates were synthesized. As a result, introducing galactose and sialic acid into CORMs, not only increased their solubility, but also improved their activity and selectivity to target molecules. Among them, complexes **1**, **8** and **10** displayed higher activities than others. Complex **1** displayed higher activities against HeLa, HePG2, MCF-7 and HT-29 cell proliferation than DDP. Its activity against HePG2 cells was about as high as 2.8 times DDP. Moreover, compared with normal cell W138, its selectivity was far better than that of DDP. Importantly, the uptake ratios of complexes **1**, **8** and **10** by the HePG2, HT-29, A549 and RAW264.7 cell lines were high. The uptake ratio of HePG2 cells for complex **1** was more than 60% after 8 h. Complex **10** was absorbed selectively by macrophage RAW264.7, and its uptake ratio was more than 50% after 8 h. Possibly, complex **1** aggregated on the surface of the cancer cell through galactose receptor selective recognition, and then entered into the HePG2 cells. Complex **10** was absorbed heavily by macrophage RAW264.7 because it has a sialic acid unit, which is selectively recognized by the sialic acid receptor. This kind of compound may have a controlling effect on immune diseases.

As for the mechanism of action, the complexes inhibited the cell cycle arrest at the G2/M phase; meanwhile, they up-regulated the expression of caspase-3 and Bax, and down-regulated Bcl-2. Of course, it also involved reducing reactive oxygen species (ROS) and lowering the mitochondrial membrane potential, and so on, like other Co-CORMs reported before.[21]

The complex containing galactose or sialic acid showed better solubility and higher selectivity to target cells, but to determine whether they can be used as candidates in clinics or not, there is a lot of further research to do.

# 4. Experimental

## 4.1. Reagents and instruments

Myoglobin (AR, Sigma), monosaccharides (Sigma), thiourea (Sigma), ytterbium(III) trifluoromethanesulfonate (Sigma), Annexin V-FITC (BD Bio-Pharmingen), PI (BD Bio-Pharmingen), and deionized water were used. All reactions were carried out under a nitrogen atmosphere. Solvents for reactions were degassed. Column chromatography was carried out using 200–300 mesh silica gel; HeLa cells, HepG2 cells, MCF-7 cells, A549 cells, HT-29 cells and W138 cell lines were purchased from the cell resources (Center for Shanghai Life Science Institute of Chinese Academy of Sciences, China). IR spectra were recorded on a Nicolet NEXUS 360 spectrophotometer, and NMR spectra on a Bruker AM-400 MHz spectrometer; a Lambda 25 UV-visible spectrophotometer and a Maxis-4G TOF mass spectrometer (ESI) were used; BD FACSverse™ flow cytometry was used for cell cycle arrest and apoptosis.

## 4.2. Synthesis of the complexes

**4.2.1. Complex 1.** $\mathbf{A_1}$ galactose (180.2 mg, 1 mmol) was dissolved in pyridine (2 mL); acetic anhydride (2 mL) was added to the mixture solution. The mixture was stirred at ambient temperature for several hours. TLC analyses (petroleum ether/AcOEt 1/1 v/v) showed complete conversion of the substrate, and the mixture was diluted with ethyl acetate. Then ice was added to the solution. The organic layer was washed with 0.5N HCl aq and $NaHCO_3$-saturated aqueous solutions, repeatedly. The organic layer was dried with anhydrous $MgSO_4$, filtered and the solvent was removed. The product was purified using column chromatography with silica gel (petroleum ether/AcOEt 3/1 v/v). Peracetylated galactose (358.2 mg) was obtained as a white solid. Yield: 65.8%. $^1$H NMR ($CDCl_3$) $\delta$ 5.69 (d, $J$ = 8.3 Hz, 1H), 5.41 (d, $J$ = 3.3 Hz, 1H), 5.11–5.06 (m, 1H), 4.13 (t, $J$ = 6.7 Hz, 2H), 4.04 (t, $J$ = 6.6 Hz, 1H), 2.15 (s, 3H), 2.11 (s, 3H), 2.03 (s, 6H), 1.99 (s, 3H). ESI-HRMS ($m/z$): calcd for $C_{16}H_{22}NaO_{11}$ $[M + Na]^+$ 413.1060, found 413.1012; $C_{16}H_{22}KO_{11}$ $[M + K]^+$ 429.0799, found 429.0746.

To a solution of peracetylated galactose (1.0 mmol) in anhydrous acetonitrile was added thiourea (1.1 mmol) and boron trifluoride diethyl etherate (2.1 mmol). The reaction mixture was refluxed until the starting material was consumed completely, and then left to cool to rt. Propargyl bromide (1.1 mmol) and triethylamine (4.5 mmol) were added and the solution was stirred at rt overnight. The reaction mixture was concentrated and the residue was diluted in $CH_2Cl_2$ before washing with aqueous 5% HCl and brine, and then filtered and evaporated. The residue was purified by phase chromatography (petroleum ether/AcOEt 5/1 v/v). $\mathbf{B_1}$ was obtained as a yellow oil. $^1$H NMR ($CDCl_3$-$d$) $\delta$ 5.38 (d, $J$ = 2.7 Hz, 1H), 5.18 (t, $J$ = 10.0 Hz, 1H), 5.04 (dd, $J$ = 10.0, 3.3 Hz, 1H), 4.70 (d, $J$ = 10.0 Hz, 1H), 4.07 (td, $J$ = 11.1, 5.8 Hz, 2H), 3.98–3.89 (m, 1H), 3.51 (dd, $J$ = 16.5, 2.5 Hz, 1H *SCH*$_2$), 3.26 (dd, $J$ = 16.5, 2.6 Hz, 1H, *SCH*$_2$), 2.25 (t, $J$ = 2.5 Hz, 1H, *CH*), 2.09 (s, 3H, *COCH*$_3$), 1.98 (s, 3H, *COCH*$_3$), 1.97 (s, 3H, *COCH*$_3$), 1.92 (s, 3H, *COCH*$_3$). ESI-HRMS ($m/z$): calcd for $C_{17}H_{22}NaO_9S$ $[M + Na]^+$ 425.0882, found 425.0851.

Then $\mathbf{B_1}$ (402.1 mg, 1 mmol) was dissolved in 2 mL of 0.5 M NaOMe in MeOH. The pH was 12 and 13. The mixture was stirred at ambient temperature for 15 min, and TLC analyses on the mixture (petroleum ether/AcOEt 1/1 v/v) showed complete conversion of the substrate. Then Amberlite® IR120 $H^+$ was added until pH 7. The resin was filtered off and the solvent was removed *in vacuo*, and the crude product was obtained. The crude product was dissolved in 20 mL of dry THF, and then 456 mg (1.2 mmol) of dicobaltoctacarbonyl was added. The reaction mixture was stirred for 12 h at room temperature. The solvent was removed *in vacuo*, the residue was extracted with a small amount of $CH_2Cl_2$, and the extract was subjected to silica gel column chromatography. Ethyl acetate/hexane (1 : 10) eluted the main red band, from which 353.6 mg (68.2%) of brown-red oil was obtained. Yield: 75.8%, IR (KBr disk, $cm^{-1}$): 2098vs, 2055vs, 2024vs (Co–CO); $[\alpha]_D^{23.7}$ −89.8° ($c$ = 1.0, $CH_3OH$), $^1$H NMR ($CDCl_3$-$d$) $\delta$ 6.08 (s, 1H, *CH*), 5.32 (m, 2H, *SCH*$_2$), 4.71–3.83 (m, 7H, *C*$_{1-5}$*H and CH*$_2$ *of sugar*), 3.41–2.573 (m, 4H, 4OH); $^{13}$C NMR (DMSO-$d_6$) $\delta$ 200.1 (Co–C), 85.6, 79.6, 79.2, 78.9, 75.3, 70.4, 68.7, 60.8, 33.4($CH_3$); ESI-HRMS ($m/z$): calcd for $C_{15}H_{16}Co_2O_{12}S$ $[M + H_2O]^+$ 537.9026, found 538.9066; $C_{15}H_{14}Co_2NaO_{11}S$ $[M + Na]^+$ 542.8819, found 542.8818; $C_{15}H_{14}Co_2KO_{11}S$ $[M + K]^+$ 558.8558, found 558.8566. Elemental anal., calcd for $C_{15}H_{14}Co_2O_{11}S$: C, 34.63; H, 2.71%, found C, 34.43, H, 2.81%.

Complex **Ac-1**: 402.1 mg (1.0 mmol) $\mathbf{B_1}$ was dissolved in 20 mL of dry THF, and then 456 mg (1.2 mmol) of dicobaltoctacarbonyl was added. The reaction mixture was stirred for 12 h at room temperature. The solvent was removed *in vacuo*, the residue was extracted with a small amount of $CH_2Cl_2$, and the extract was subjected to silica gel column chromatography. Ethyl acetate/hexane (1 : 10) eluted the main red band, from which 590.8 mg (86.1%) of complex **Ac-1** as a brown-red oil was obtained. IR (KBr disk, $cm^{-1}$): 2099vs, 2054vs, 2018vs, 1753vs, (COO); $[\alpha]_D^{21.5}$ −79.1° ($c$ = 1.0, $CH_3OH$), $^1$H NMR ($CDCl_3$) $\delta$ 6.03 (s, 1H, *CH*), 5.23 (s, 2H, *SCH*$_2$), 5.03–3.69 (m, 7H, $C_{1-5}$H and $CH_2$ of sugar), 1.96 (br, 12H, *COCH*$_3$); $^{13}$C NMR ($CDCl_3$) $\delta$ 198.3 (Co–C), 169.5 (CO), 169.1 (CO), 168.4 (CO), 90.6, 81.9, 75.2, 72.8, 72.6, 68.7, 67.2, 61.1, 32.4 ($SCH_2$), 19.6 ($CH_3$); ESI-HRMS ($m/z$): calcd for $C_{23}H_{22}Co_2NaO_{15}S$ $[M + Na]^+$ 710.9241, found 710.9229; $C_{23}H_{22}Co_2KO_{15}S$ $[M + K]^+$ 726.8980, found 726.8968. Elemental anal., calcd for $C_{23}H_{22}Co_2O_{15}S$: C, 40.13; H, 3.22%, found C, 40.03, H, 3.34%.

The procedure and workup of complexes **2–7** were similar to the process of complex **1** and the procedure and workup of complexes **Ac-2–Ac-7** were similar to the process of complex **Ac-1**.

**4.2.2. Complex 2.** Yield: 77.8%; IR (KBr disk, $cm^{-1}$): 2099vs, 2051vs, 2024vs (Co–CO); $[\alpha]_D^{22.5}$ −68.9° ($c$ = 1.0, $CH_3OH$), $^1$H NMR ($CDCl_3$) $\delta$ 6.06 (s, 1H, CH), 5.30 (m, 2H, $SCH_2$), 4.52–3.66 (m, 7H, $C_{1-5}$H and $CH_2$ of sugar), 3.36–2.51 (m, br, 4H, 4OH). $^{13}$C NMR (DMSO-$d_6$) $\delta$ 199.1 (Co–C), 86.6,

78.6, 78.2, 77.9, 74.3, 70.4, 68.7, 61.8, 33.6; ESI-HRMS (*m*/*z*): calcd for $C_{15}H_{15}Co_2O_{11}S$ $[M + H]^+$ 520.8999, found 520.9671; $C_{15}H_{16}Co_2O_{12}S$ $[M + H_2O]^+$ 537.9026, found 538.9262; $C_{15}H_{14}Co_2NaO_{11}S$ $[M + Na]^+$ 542.8819, found 542.8818; $C_{15}H_{14}Co_2KO_{11}S$ $[M + K]^+$ 558.8558, found 558.8555. Elemental anal., calcd for $C_{15}H_{14}Co_2O_{11}S$, C, 34.63; H, 2.71%, found C, 34.80, H, 2.89%.

Complex **Ac-2**: Yield: 67.8%; IR (KBr disk, $cm^{-1}$): 2091vs, 2053vs, 2034vs, 1851vs, (COO); $[\alpha]_D^{20.5}$ −48.3° (*c* = 1.0, $CH_3OH$), $^1H$ NMR ($CDCl_3$) *δ* 6.02 (s, 1H, *CH*), 5.24 (s, 2H, $SCH_2$), 5.06–3.68 (m, 7H, *$C_{1\text{-}5}H$ and $CH_2$ of sugar*), 1.98 (s, 12H, *$COCH_3$*). $^{13}C$ NMR ($CDCl_3$) *δ* 199.3 (Co–C), 169.8 (CO), 169.3 (CO), 168.0 (CO), 85.6, 81.9, 75.2, 72.8, 72.6, 68.7, 66.2, 60.1, 32.8 ($SCH_2$), 19.9 ($CH_3$); ESI-HRMS (*m*/*z*): calcd for $C_{23}H_{22}Co_2NaO_{15}S$ $[M + Na]^+$ 710.9241, found 710.9231. Elemental anal., calcd for $C_{23}H_{22}Co_2O_{15}S$: C, 40.13; H, 3.22%, found C, 40.21, H, 3.39%.

**4.2.3. Complex 3.** Yield: 68.1%; IR (KBr disk, $cm^{-1}$): 2099vs, 2054vs, 2045vs (Co–CO); $[\alpha]_D^{22.7}$ −100.2° (*c* = 1.0, $CH_3OH$), $^1H$ NMR ($CDCl_3$) *δ*6.05 (s, 1H, *CH*), 5.46–5.26 (m, 2H, *$SCH_2$*), 5.26–3.88 (m, 5H, *$C_{1\text{-}5}H$ of sugar*), 3.72 (s, 3H, *$OCH_3$*), 3.25–2.23 (m, 3H, *3OH*). $^{13}C$ NMR (DMSO-*$d_6$*) *δ* 199.3 (Co–C), 170.3, 94.5, 85.1, 76.4, 72.9, 68.3, 53.6, 32.6; ESI-HRMS (*m*/*z*): calcd for $C_{15}H_{14}Co_2NaO_{11}S$ $[M + Na]^+$ 570.8768, found 570.8766; $C_{16}H_{14}Co_2KO_{12}S$ $[M + K]^+$ 586.8507, found 586.8512. Elemental anal., calcd for $C_{16}H_{14}Co_2O_{12}S$: C, 35.06; H, 2.57%, found C, 35.18, H, 2.71%.

Complex **Ac-3**: Yield: 80.4%; IR (KBr disk, $cm^{-1}$): 2091vs, 2055vs, 2047vs, 1750vs (COO); $[\alpha]_D^{23.2}$ −153.6° (*c* = 1.0, $CH_3OH$), $^1H$ NMR ($CDCl_3$) *δ*6.04 (s, 1H, *CH*), 5.13 (br, 2H, *$SCH_2$*), 4.60–4.05 (m, 5H, *$C_{1\text{-}5}H$ of sugar*), 3.69 (s, 3H, *$OCH_3$*), 1.96 (s, 9H, *$COCH_3$*). $^{13}C$ NMR ($CDCl_3$) *δ*199.2, 169.9, 169.3, 166.7, 91.8, 83.3, 76.4, 73.0, 69.4, 52.9, 33.6, 20.5; ESI-HRMS (*m*/*z*): calcd for $C_{22}H_{20}Co_2NaO_{15}S$ $[M + Na]^+$ 696.9085, found 696.9056. Elemental anal., calcd for $C_{22}H_{20}Co_2O_{15}S$: C, 39.19; H, 2.99%, found C, 39.04, H, 3.08%.

**4.2.4. Complex 4.** Yield: 83.1%; IR (KBr disk, $cm^{-1}$): 2093vs, 2057vs, 2022vs (Co–CO); $[\alpha]_D^{23.4}$ 340.8° (*c* = 1.0, $CH_3OH$), $^1H$ NMR ($CDCl_3$) *δ*6.85 (s, 1H, *CH*), 5.18 (m, 2H, *$SCH_2$*), 4.85–3.88 (m, 7H, *$C_{1\text{-}5}H$ of sugar and $CH_2$*), 3.67–3.34 (m, 4H, *4OH*). $^{13}C$ NMR (DMSO-*$d_6$*) *δ* 200.3 (Co–C), 94.5, 85.1, 75.4, 71.9, 67.3, 49.06, 33.4; ESI-HRMS (*m*/*z*): calcd for $C_{15}H_{14}Co_2NaO_{11}S$ $[M + Na]^+$ 542.8819, found 542.8842. $C_{15}H_{14}Co_2KO_{11}S$ $[M + K]^+$ 558.8558, found 558.8560. Elemental anal., calcd for $C_{15}H_{14}Co_2O_{11}S$, C, 34.63; H, 2.71%, found C, 34.82, H, 2.88%.

Complex **Ac-4**: Yield: 85.0%; IR (KBr disk, $cm^{-1}$): 2097vs, 2049vs, 2024vs, 1753vs (COO); $[\alpha]_D^{22.6}$ 178.1° (*c* = 1.0, $CH_3OH$), $^1H$ NMR ($CDCl_3$) *δ* 6.08 (br, 1H, *CH*), 5.39 (m, 2H, $SCH_2$), 4.87–3.95 (m, 7H, *$C_{1\text{-}5}H$ and $CH_2$ of sugar*), 2.12 (br, 3H, *$COCH_3$*), 2.02 (br, 3H, *$COCH_3$*), 1.98 (br, 3H, *$COCH_3$*), 1.93 (s, 3H, *$COCH_3$*). $^{13}C$ NMR (DMSO-*$d_6$*) *δ* 198.2 (Co–C), 170.1, 169.6, 169.0, 168.7 (C═O), 85.6, 79.6, 79.2, 78.9, 75.3, 70.4, 68.7, 60.8, 33.4; ESI-HRMS (*m*/*z*): calcd for $C_{23}H_{22}Co_2KO_{15}S$ $[M + K]^+$ 726.8980, found 726.8906. Elemental anal., calcd for $C_{23}H_{22}Co_2O_{15}S$: C, 40.13; H, 3.22%, found C, 40.24, H, 3.37%.

**4.2.5. Complex 5.** Yield: 80.1%; IR (KBr disk, $cm^{-1}$): 2092vs, 2058vs, 2034vs (Co–CO); $[\alpha]_D^{23.5}$ 127.3° (*c* = 1.0, $CH_3OH$), $^1H$ NMR ($CDCl_3$) *δ* 6.05 (s, 1H, *CH*), 5.31 (m, 2H, $SCH_2$), 4.90–3.56 (m, 7H, $C_{2\text{–}4}H$ and $CH_2$ of sugar), 3.42–3.06 (m, 4H, 4OH). $^{13}C$ NMR (DMSO-$d_6$) *δ* 199.9 (Co–C), 85.1, 76.4, 72.9, 68.3, 65.3, 61.2, 53.6, 32.6. ESI-HRMS (*m*/*z*): calcd for $C_{15}H_{14}Co_2NaO_{11}S$ $[M + Na]^+$ 542.8819, found 542.8849. Elemental anal., calcd for $C_{15}H_{14}Co_2O_{11}S$: C, 34.63; H, 2.71%, found C, 34.44, H, 2.86%.

Complex **Ac-5**: Yield: 79.6%; IR (KBr disk, $cm^{-1}$): 2095vs, 2048vs, 2019vs, 1749vs (COO); $[\alpha]_D^{20.5}$ 97.3° (*c* = 1.0, $CH_3OH$), $^1H$ NMR ($CDCl_3$) *δ* 6.02 (s, 1H, *CH*), 5.56 (m, 2H, $SCH_2$), 4.92–4.07 (m, 7H, $C_{2\text{–}4}H$ and $CH_2$ of sugar), 2.02 (s, 12H, $COCH_3$). $^{13}C$ NMR ($CDCl_3$) *δ* 199.1, 170.4, 170.0, 168.9, 80.8, 79.8, 79.2, 78.0, 77.2, 76.8, 73.6, 65.0, 62.7, 32.5, 20.7; ESI-HRMS (*m*/*z*): calcd for $C_{23}H_{22}Co_2NaO_{15}S$ $[M + Na]^+$ 710.9241, found 710.9237. Elemental anal., calcd for $C_{23}H_{22}Co_2O_{15}S$: C, 40.13; H, 3.22%, found C, 40.24, H, 3.37%.

**4.2.6. Complex 6.** Yield: 77.2%; IR (KBr disk, $cm^{-1}$): 2097vs, 2054vs, 2033vs, (Co–CO), $[\alpha]_D^{20.6}$ −186.8° (*c* = 1.0, $CH_3OH$), $^1H$ NMR ($CDCl_3$) *δ* 6.10 (s, 1H, *CH*), 5.29 (s, 2H, $SCH_2$), 4.88–3.94 (m, 5H, $C_{1\text{–}5}H$ of sugar), 3.86–2.86 (m, 4H, 4OH), 1.25 (s, 3H, *$CH_3$*). $^{13}C$ NMR ($CDCl_3$) *δ* 198.3 (Co–C), 90.8, 83.2, 76.2, 72.6, 72.1, 71.2, 68.2, 33.6($SCH_2$), 16.5($CH_3$); CORM: ESI-HRMS (*m*/*z*): calcd for $C_{15}H_{14}Co_2KO_{10}S$ $[M + K]^+$ 542.8609, found 542.8914. Elemental anal., calcd for $C_{15}H_{14}Co_2O_{10}S$: C, 35.73; H, 2.80%, found C, 35.54, H, 2.93%.

Complex **Ac-6**: Yield: 83.9%; IR (KBr disk, $cm^{-1}$): 2099vs, 2051vs, (Co–CO), 1750vs, (COO); $[\alpha]_D^{21.5}$ −236.5° (*c* = 1.0, $CH_3OH$); $^1H$ NMR ($CDCl_3$) *δ*5.92 (s, 1H, *CH*), 5.22 (m, 2H, $SCH_2$), 4.91–3.88 (m, 7H, $C_{1\text{–}5}H$ and $CH_2$ of sugar), 2.09 (s, 3H, $COCH_3$), 1.99 (s, 3H, $COCH_3$), 1.92 (br, 6H, *$COCH_3$*); $^{13}C$ NMR ($CDCl_3$) *δ* 199.2, 170.4, 170.2, 169.6, 85.3, 82.8, 73.6, 72.4, 70.4, 67.2, 33.3, 20.8, 16.9; ESI-HRMS (*m*/*z*): calcd for $C_{23}H_{22}Co_2KO_{15}S$ $[M + K]^+$ 726.8980, found 726.8968. Elemental anal., calcd for $C_{21}H_{20}Co_2O_{13}S$: C, 40.02; H, 3.20%, found C, 40.11, H, 3.29%.

**4.2.7. Complex 7.** Yield: 77.6%; IR (KBr disk, $cm^{-1}$): 2095vs, 2053vs, 2030vs, (Co–CO); $[\alpha]_D^{23.1}$ −40.9° (*c* = 1.0, $CH_3OH$), $^1H$ NMR ($CDCl_3$) *δ* 6.07 (s, 1H, *CH*), 5.22 (s, 2H, $SCH_2$), 4.40–3.86 (m, 5H, $C_{1\text{–}5}H$ and $CH_2$ of sugar), 3.57–3.06 (br, 3H, 3OH), 1.22 (s, 3H, *$CH_3$*); $^{13}C$ NMR ($CDCl_3$) *δ* 199.3 (Co–C), 89.8, 81.2, 72.2, 71.6, 70.1, 69.2, 67.2, 33.9 ($SCH_2$), 16.8 ($CH_3$); ESI-HRMS (*m*/*z*): calcd for $C_{15}H_{14}Co_2NaO_{10}S$ $[M + Na]^+$ 526.8869, found 526.8862. Elemental anal., calcd for $C_{15}H_{14}Co_2O_{10}S$: C, 35.73; H, 2.80%, found C, 35.57, H, 2.95%.

Complex **Ac-7**: Yield: 85.1%; IR (KBr disk, $cm^{-1}$): 2093vs, 20516vs, 2017vs, 1755vs (COO); $[\alpha]_D^{23.2}$ −79.1° (*c* = 1.0, $CH_3OH$), $^1H$ NMR ($CDCl_3$) *δ* 6.03 (s, 1H, CH), 5.12 (m, 2H, $SCH_2$), 4.90–3.79 (m, 5H, *$C_{1\text{-}5}H$ and $CH_2$ of sugar*), 1.97 (s, 9H, *$COCH_3$*), 1.18 (s, 3H, *$CH_3$*). 5.12 (d, *J* = 88.3 Hz, 3H), 4.50 (s, 1H), 4.12 (s, 1H), 4.06 (s, 1H), 3.79 (s, 1H), 1.97 (s, 9H), 1.18 (s, 3H). $^{13}C$ NMR ($CDCl_3$) *δ* 199.4, 170.6, 170.2, 169.7, 92.3, 82.8, 73.6, 72.3, 70.4, 67.2, 33.2, 20.6, 16.3; ESI-HRMS (*m*/*z*): calcd for $C_{21}H_{20}Co_2NaO_{13}S$ $[M + Na]^+$ 652.9186, found 652.9179.

 

Elemental anal., calcd for $C_{21}H_{20}Co_2O_{13}S$: C, 40.02; H, 3.20%, found C, 40.17; H, 3.31%.

**4.2.8. Complex 8.** $A_8$ (2.00 g, 9.28 mmol) was dissolved in anhydrous pyridine (20 mL), and acetic anhydride (10.5 mL, 111.3 mmol) was added. The mixture was stirred at room temperature until the disappearance of the starting material, and poured into ice-cold water. A white solid precipitate was collected by filtration, washed with ice-cold water and co-evaporated with toluene (3 × 20 mL) to remove residual water to yield 2.96 g (82%) of powdery solid (peracetylated aminogalactose). $^1$H NMR ($CDCl_3$) $\delta$ 5.70 (d, $J$ = 8.4 Hz, 1 H), 5.40 (d, $J$ = 9.0 Hz, 1 H), 5.30 (d, $J$ = 2.5 Hz, 1 H), 5.04 (dd, $J$ = 3.0, 11.0 Hz, 1 H), 4.44–4.360 (m, 1 H), 4.20–4.08 (m, 2 H), 4.07–4.02 (m, 1H), 2.16 (s, 3 H), 2.14 (s, 3 H), 2.00 (s, 3 H), 1.98 (s, 3 H), 1.94 (s, 3H). ESI-HRMS ($m/z$): calcd for $C_{16}H_{25}NO_{11}$ $[M + H_2O]^+$ 407.1428, found 407.1458; $C_{16}H_{23}NNaO_{10}$ $[M + Na]^+$ 412.1220, found 412.1229.

Then propargyl alcohol (29.9 μL, 0.514 mmol) and $Yb(OTf)_3$ (47.8 mg, 0.231 mmol) were added to a solution of peracetylated aminogalactose (100 mg, 0.257 mmol) in dry DCE (6 mL). The solution was stirred for 24 h at 70 °C. The solution was diluted with DCM and washed with water. The organic layer was dried with sodium sulfate and concentrated *in vacuo* to furnish $\mathbf{B_8}$ (86 mg, 87%). $^1$H NMR ($CDCl_3$) $\delta$ 5.48 (d, $J$ = 8.8 Hz, 1H), 5.20 (t, $J$ = 10.0 Hz, 1H), 5.06 (t, $J$ = 9.8 Hz, 1H), 4.84 (d, $J$ = 8.4 Hz, 1H), 4.38 (s, 2H), 4.27 (dd, $J$ = 12.2, 4.6 Hz, 1H), 4.16 (d, $J$ = 12.0 Hz, 1H), 3.90 (dd, $J$ = 18.6, 9.2 Hz, 1H), 3.70 (d, $J$ = 9.8 Hz, 1H), 2.43 (d, $J$ = 1.3 Hz, 1H), 2.11–1.96 (m, 12H). ESI-HRMS ($m/z$): calcd for $C_{17}H_{25}NO_{10}$ $[M + H_2O]^+$ 403.1478, found 403.1408; $C_{17}H_{23}NNaO_9$ $[M + Na]^+$ 408.1271, found 408.1287.

Then $\mathbf{B_8}$ was dissolved in 2 mL of 0.5 M NaOMe in MeOH. The pH was between 12 and 13. The mixture was stirred at ambient temperature for 15 min, and TLC analyses (petroleum ether/AcOEt 1/1 v/v) showed complete conversion of the substrate. Then Amberlite® IR120 $H^+$ was added until pH 7 was reached; the resin was filtered off and the solvent was removed *in vacuo*, the crude product was obtained, then the crude product was dissolved in 20 mL of dry THF, and then dicobaltoctacarbonyl was added. The reaction mixture was stirred for 12 h at room temperature. The solvent was removed *in vacuo*, the residue was extracted with a small amount of $CH_2Cl_2$, and the extract was subjected to silica gel column chromatography. Ethyl acetate/hexane (1 : 6) eluted the main red band, and complex **8** was obtained (yield 68.2%), IR (KBr disk, $cm^{-1}$): 2094vs, 2054vs, 2019vs (Co–CO), 1686vs (CON); $[\alpha]_D^{23.3}$ 57.2° ($c$ = 1.0, $CH_3OH$); $^1$H NMR ($CDCl_3$) $\delta$ 5.86 (s, 1H, CH), 5.04 (s, 2H, $OCH_2$), 4.82–3.94 (m, 8H, $C_{1-5}$H of sugar, $CH_2$, NH), 3.51–2.26 (m, 3H, 3OH), 1.84 (s, 3H, $CH_3$). $^{13}$C NMR (DMSO-$d_6$) $\delta$ 200.1 (Co–C), 85.6, 79.6, 79.2, 78.9, 75.3, 70.4, 68.7, 60.8, 33.4($CH_3$); ESI-HRMS ($m/z$): calcd for $C_{17}H_{17}Co_2NNaO_{12}$ $[M + Na]^+$ 567.9312, found 567.9626. Elemental anal., calcd for $C_{17}H_{17}Co_2NO_{12}$: C, 37.45; H, 3.14%, found C, 37.57; H, 3.31%.

Complex **Ac-8**: $\mathbf{B_8}$ was dissolved in 20 mL of dry THF, and then dicobaltoctacarbonyl was added. The reaction mixture was stirred for 12 h at room temperature. The solvent was removed *in vacuo*, the residue was extracted with a small amount of $CH_2Cl_2$, and the extract was subjected to silica gel column chromatography. Ethyl acetate/hexane (1 : 10) eluted the main red band, and complex **Ac-8** as a brown-red oil was obtained (86.1%). IR (KBr disk, $cm^{-1}$): 2099vs, 2052vs, 2021vs, 1747vs (COO), 1687s (CON); $[\alpha]_D^{23.8}$77.1 ($c$ = 1.0, $CH_3OH$), $^1$H NMR ($CDCl_3$) $\delta$5.99 (s, 1H, *CH*), 5.51 (s, 2H, $OCH_2$), 4.90–3.63 (m, 8H, $C_{1-5}$H of sugar, $CH_2$, NH), 2.33–1.64 (m, 12H, *$COCH_3$*). $^{13}$C NMR ($CDCl_3$) $\delta$ 199.5, 198.3, 198.2 (Co–C), 169.6, 169.2, 168.5 (C═O), 98.29, 71.08, 70.93, 70.88, 67.94, 67.75, 61.09, 54.38, 22.24 ($CH_3$), 19.66($CH_3$); ESI-HRMS ($m/z$): calcd for $C_{23}H_{23}Co_2KNO_{15}$ $[M + K]^+$ 709.9369, found 709.9757. Elemental anal., calcd for $C_{23}H_{23}Co_2NO_{15}$: C, 41.15; H, 3.45%, found C, 41.01; H, 3.56%.

The procedure and workup of complex **9** were similar to the process of complex **8** and the procedure and workup of complexes **Ac-9** were similar to the process of complex **Ac-8**.

**4.2.9. Complex 9.** Yield: 65.1%; IR (KBr disk, $cm^{-1}$): 2096vs, 2059vs, 2033vs (Co–CO), 1683s (CON). $[\alpha]_D^{23.7}$ −73.8° ($c$ = 1.0, $CH_3OH$), $^1$H NMR ($CDCl_3$) $\delta$ 5.82 (s, 1H, *CH*), 5.10 (s, 2H, $OCH_2$), 4.80–3.86 (m, 8H, *$C_{1\text{-}5}H$ of sugar*, *$CH_2$*, *NH*), 3.70–3.35 (m, 3H, *3OH*), 2.02 (s, 3H, *$CH_3$*). $^{13}$C NMR ($CDCl_3$) $\delta$200.1 (Co–C), 169.9, 81.0, 72.9, 71.0, 70.4, 69.5, 67.3, 35.6 ($SCH_2$), 19.5; ESI-HRMS ($m/z$): calcd for $C_{17}H_{17}Co_2NNaO_{12}$ $[M + Na]^+$ 567.9312, found 567.3191. Elemental anal., calcd for $C_{17}H_{17}Co_2NO_{12}$: C, 37.45; H, 3.14%, found C, 37.55; H, 3.33%.

Complex **Ac-9**: Yield: 75.1%; IR (KBr disk, $cm^{-1}$): 2091vs, 2055vs, 2047vs, 1750vs (COO), 1684s (CON); $[\alpha]_D^{23.9}$ −117.3° ($c$ = 1.0, $CH_3OH$), $^1$H NMR ($CDCl_3$) $\delta$ 6.02 (br, 1H, *CH*), 5.60 (s, 2H, $OCH_2$), 4.78–3.58 (m, 8H, *$C_{1\text{-}5}H$ of sugar*, *$CH_2$*, *NH*), 2.36–1.68 (m, 12H, *$COCH_3$*). $^{13}$C NMR ($CDCl_3$) $\delta$ 201.6, 198.3, 198.2 (Co–C), 169.6, 169.1, 169.5 (C═O), 98.3, 71.2, 70.9, 70.8, 67.8, 67.6, 61.1, 54.4, 22.2 ($CH_3$), 19.6($CH_3$); ESI-HRMS ($m/z$): calcd for $C_{23}H_{23}Co_2KNO_{15}$ $[M + K]^+$ 709.9369, found 709.9357. Elemental anal., calcd for $C_{23}H_{23}Co_2NO_{15}$: C, 41.15; H, 3.45%, found C, 41.00; H, 3.66%.

**4.2.10. Complex 10.** *N*-Acetylneuraminic acid (5.07 g, 16.4 mmol) dissolved in dry MeOH (100 mL) with a strong cation-exchange resin (Dowex 50W-X2) ($H^+$) (5.08 g) was stirred at rt under $N_2$ gas. After the reaction mixture had been stirred for 48 h, the cation-exchange resin was removed and the MeOH solution was concentrated. To a solution of the residue in dry pyridine (100 mL) was added $Ac_2O$ (125 mL, 1.32 mmol), and then stirred at rt in the dark for 20 h. The solution was concentrated to remove pyridine and acetic acid. The crude product was purified by column chromatography on silica gel ($CHCl_3$–isopropanol 50 : 1 → 3 : 1) to afford penta-*O*-acetyl-*N*-acetylneuraminic acid methyl ester (72%). $^1$H NMR ($CDCl_3$): $\delta$ 6.22 (d, $J$ = 8.9 Hz, 1H), 5.35 (d, $J$ = 4.4 Hz, 1H), 5.18 (s, 1H), 5.00 (s, 1H), 4.46 (d, $J$ = 14.6 Hz, 1H), 4.34 (dd, $J$ = 12.4, 2.5 Hz, 0H), 4.12 (d, $J$ = 5.7 Hz, 2H), 3.71 (d, $J$ = 13.7 Hz, 3H), 2.48 (dd, $J$ = 13.4, 4.9 Hz, 1H), 2.11–1.93 (m, 15H), 1.82 (s, 3H). ESI-HRMS ($m/z$): calcd for $C_{22}H_{31}NNaO_{14}$ $[M + Na]^+$ 556.1642, found 556.1612.

Then propargyl alcohol (29.9 μL, 0.514 mmol) and $Yb(OTf)_3$ (47.8 mg, 0.231 mmol) were added to a solution of penta-*O*-acetyl-*N*-acetylneuraminic acid methyl ester (136 mg, 0.257 mmol) in dry DCE (6 mL). The solution was stirred for 24 h at 70 °C. The solution was diluted with DCM and washed with water. The organic layer was dried with sodium sulfate and concentrated *in vacuo* to furnish **$B_{10}$** (85 mg, 82%). $^1$H NMR ($CDCl_3$) $\delta$ 5.40 (s, 1H), 5.32 (s, 1H), 5.24–5.18 (m, 1H), 4.86 (s, 1H), 4.39 (s, 1H), 4.28 (s, 1H), 4.15 (s, 1H), 4.11–4.02 (m, 3H), 3.76 (s, 3H), 2.58 (dd, $J$ = 12.8, 4.6 Hz, 1H), 2.40 (t, $J$ = 2.4 Hz, 1H), 2.18–1.80 (m, 15H), 2.06–1.90 (m, 1H).

Then **$B_{10}$** was dissolved in 2 mL of 0.5 M NaOMe in MeOH. The pH was between 12 and 13. The mixture was stirred at ambient temperature for 15 min, and TLC analyses on the mixture (petroleum ether/AcOEt 1/1 v/v) showed complete conversion of the substrate. Then Amberlite® IR120 $H^+$ was added until pH 7 was reached. The resin was filtered off and the solvent was removed *in vacuo*, and the crude product was obtained. The crude product was dissolved in 20 mL of dry THF, and then dicobaltoctacarbonyl was added. The reaction mixture was stirred for 12 h at room temperature. The solvent was removed *in vacuo*, the residue was extracted with a small amount of $CH_2Cl_2$, and the extract was subjected to silica gel column chromatography. Ethyl acetate/hexane (1 : 4) eluted the main red band, and complex **10** was obtained (yield 68.2%). $[\alpha]_D^{22.7}$ −34.3°($c$ = 1.0, $CH_3OH$), IR (KBr disk, $cm^{-1}$): 2097vs, 2052vs, 2033vs, 2024vs (Co–CO); $^1$H NMR ($CDCl_3$) $\delta$ 6.01 (br, 1H, *CH*), 5.36 (br 2H, $OCH_2$), 4.79–3.88 (m, 10H, $C_{2-5}H$ of sugar, $CH_2$, CH, NH), 3.75 (br, 3H, *$OCH_3$*), 3.65–2.89 (m, 4H, *4OH*), 2.09 (s, 3H, *$CH_3$*); $^{13}$C NMR ($CDCl_3$) $\delta$ 198.5 (Co–C), 198.2 (Co–C), 169. 6 (CO), 169.3 (CO), 97.9, 88.6, 71.5, 71.5, 70.5, 67.6, 67.5, 65.0, 61.4, 51.8, 48.3, 36.3, 22.2; ESI-HRMS ($m/z$): calcd for $C_{21}H_{23}Co_2KNO_{15}$ $[M + K]^+$ 685.9369, found 685.9314. Elemental anal., calcd for $C_{21}H_{23}Co_2NO_{15}$: C, 38.97; H, 3.58%, found C, 39.05; H, 3.66%.

Complex **Ac-10**: **$B_{10}$** was dissolved in 20 mL of dry THF, and then dicobaltoctacarbonyl was added. The reaction mixture was stirred for 12 h at room temperature. The solvent was removed *in vacuo*, the residue was extracted with a small amount of $CH_2Cl_2$, and the extract was subjected to silica gel column chromatography. Ethyl acetate/hexane (1 : 6) eluted the main red band, complex **Ac-10**, as a brown-red oil was obtained (86.1%). $[\alpha]_D^{20.7}$ −10.6°($c$ = 1.0, $CH_3OH$); IR (KBr disk, $cm^{-1}$): 2098vs, 2056vs, 2034vs, 1745vs (COO); $^1$H NMR ($CDCl_3$) $\delta$ 6.02 (s, 1H, *CH*), 5.35 (br, 2H, $OCH_2$), 4.85–3.98 (br, 10H, $C_{2-5}H$ of *sugar*, *$CH_2$*, *CH*, *NH*), 3.75 (s, 3H, *$OCH_3$*), 2.09–1.81 (m, 15H, *$COCH_3$ and $CNCH_3$*). $^{13}$C NMR ($CDCl_3$) $\delta$ 198.5 (Co–C), 198.2 (Co–C), 169.8 (CO), 169.7 (CO), 169, 6 (CO), 169.3 (CO), 169.2 (CO), 166.1 (CO), 97.9, 88.6, 71.5, 71.5, 70.5, 67.6, 67.5, 65.0, 61.4, 51.8, 48.3, 36.3, 22.2, 20.0, 19.8, 19.8, 19.7; ESI-HRMS ($m/z$): calcd for $C_{29}H_{32}Co_2NO_{19}$ $[M + H]^+$ 816.0233, found 816.0679; $C_{29}H_{33}Co_2NO_{20}$ $[M + H_2O]^+$ 833.0260, found 833.0952; $C_{29}H_{31}Co_2NNaO_{19}$ $[M + Na]^+$ 838.0052, found 838.0509. Elemental anal., calcd for $C_{29}H_{31}Co_2NO_{19}$: C, 42.72; H, 3.83%, found C, 42.58; H, 3.99%.

### 4.3. Lipophilicity (log *P* o/w)

The lipophilicity of the complex was determined using the flask shaking method where *n*-octanol and 0.1 M PBS were used as the organic and aqueous phases respectively. *n*-Octanol was presaturated with 0.1 M PBS by swirling at 45 rpm for 24 h. The test complex was dissolved in the isolated organic phase at a concentration of 50 μM. An equal volume of aqueous PBS was added, and the mixture was swirled for 8 h at 45 rpm at 37 °C. The solution was then centrifuged, and the amounts of complex in both layers were determined by ICP-AES, and then log *P* was calculated.

### 4.4. CO-release tests with myoglobin assay

The release of CO from the metal carbonyl complexes was studied spectrophotometrically by measuring the conversion of deoxy-myoglobin (deoxy-Mb) to carbonyl myoglobin (Mb-CO). The amount of Mb-CO formed was quantified by measuring the absorbance at 540 nm. A stock solution of myoglobin (lyophilised horse heart) (60 μM final concentration) was prepared fresh by dissolving the protein in phosphate buffered saline (PBS, 0.1 M, pH = 7.4). Sodium dithionite (0.1%) was added to convert the myoglobin stock to deoxy-Mb. A 2 ml quantity of this solution was assayed to obtain a deoxy-Mb spectrum and then bubbled with CO to obtain an Mb-CO spectrum. Each complex was dissolved in water and added to deoxy-Mb in the cuvette, mixed using a pipette and then overlaid with 500 μL light mineral oil to prevent CO from escaping or the myoglobin from being oxygenated. This is the standard procedure; other experiments have been undertaken using different concentrations of myoglobin.

In these experiments, the absorption peak of deoxy-Mb at 560 nm was replaced by the two peaks of Mb-CO at 540 and 578 nm. The concentration of myoglobin in the stock solution was calculated from the absorption maximum of the Mb-CO solution at 540 nm.

### 4.5. Cytotoxicity assays

HeLa cells, HepG2 cells, MCF-7 cells, A549 cells, HT-29 cells and W138 cell lines were purchased from cell resources (Center for Shanghai Life Science Institute of Chinese Academy of Sciences, China). The cells were cultivated at 37 °C, 10% $CO_2$, 100% humidity in RPMI1640 medium, enriched with glucose and supplemented with 10% fetal bovine serum, non-essential amino acids, antibiotics (penicillin/streptomycin) and antifungals. Typically, 8 μmol of the complex was dissolved in 1.0 mL of culture medium with vigorous stirring. The growth inhibitory effect toward the cell line was determined by means of the MTT colorimetric assay. The cells (100 μL, $1 \times 10^5$ cells per mL) were seeded into 96-well plates and left to adhere for 24 h. The media were removed from the wells and replaced with fresh media containing the complexes of different concentrations (3.25, 6.5, 12.5, 25, 50, 100, 200 and 400 μmol $L^{-1}$), respectively. The cells were then incubated for another 24 h before the incubation media were

 

$$\text{Uptake ratio}\,(\%) = \frac{(\text{find Co in cell lysate}) \times (\text{volume of cell lysate})}{(\text{find Co in cell lysate}) \times (\text{volume of cell lysate}) + (\text{find Co in medium}) \times (\text{volume of medium})}$$

replaced with the complete medium and MTT (10 μL, 5 mg $mL^{-1}$ in phosphate buffered saline, PBS) was added to each well of the plate. The cells were further incubated for 4 h before the media were replaced with DMSO (100 μL). Absorbance at 490 nm for each well of the plates was recorded with a microplate reader. In the MTT assay, DMSO (100 μL) in a well was used as a blank and the cells in the well without the addition of any complexes were taken as a control (100% cell viability).

### 4.6. Cellular uptake

Cancer cells were grown until at least 70% confluency in 75 $cm^2$ cell-culture flasks. Stock solutions of the compounds in DMSO were prepared and diluted in cell-culture medium to a final concentration of 100 μM immediately before use (final DMSO concentration: 0.1% v/v). The cell-culture medium of the flasks was replaced with the medium that contained the metal compound (10 mL) and the flasks were incubated at 37 °C/5% $CO_2$ for 2 h, 4 h and 8 h. After the desired incubation period the uptake was stopped by removing the cell-culture medium. The pellet cells were washed with sterilized 10 mM PBS (pH 7.4) and centrifuged to obtain cell pellets. The pellets were lysed with 10% Tween 20 (50 μL). The concentration of Co atoms in the cell lysate was measured by ICP-MS. The percentage of uptake was calculated from the amount of Co atoms in culture medium and in the cell lysates using the following equation.

### 4.7. Flow cytometry assays

The HePG2 cell lines were cultured at 37 °C, 5% $CO_2$, 100% humidity in RPMI 1640 medium supplemented with 10% fetal bovine serum. The cells were cultured in 6-well plates for 24 h. The media were removed from the wells and treated with various concentrations of complexes **1**, **8** or **10** for 24 h. The control cells were treated with vehicle. Next, the cells were detached using 0.25% trypsin-EDTA (0.5 ml) and then resuspended in media (4 ml) prior to centrifugation (1000 rpm for 5 min). Cell pellets were washed twice using PBS (2 ml). For cell-cycle analysis, the cells were fixed in cold 70% ethanol, RNase treated, and stained with propidium iodide (PI) in the dark for 30 min at 37 °C. The cells were analyzed for their DNA content by BD FACSverse™ flow cytometry. For apoptosis analysis, the cells were stained with Annexin V-FITC (BD Bio-Pharmingen) and PI in the dark for 15 min. The percentages of apoptotic cells were determined by BD FACSverse™ flow cytometry for 1 h.

### 4.8. Western blotting analysis

HepG2 cells were seeded into culture flasks. After 24 h incubation, the cells were treated with complex **1** (0, 10, and 20 μM), respectively. For total cell protein extracts, the cells were washed and lysed in lysis buffer (50 mM Tris-HCl (pH 7.5), 1% NP-40, 2 mM EDTA, 10 mM NaCl, 10 μg $ml^{-1}$ aprotinin, 10 μg $ml^{-1}$ leupeptin, 1 mM DTT, 0.1% SDS and 1 mM phenyl methyl sulfonyl fluoride). Total proteins were obtained by centrifugation (12 000*g* for 20 min at 4 °C). The protein concentrations were determined by using the Bradford method. For western blot analysis, equal amounts of proteins (30 μg) were separated on 10% or 12% SDS-PADE gels and transferred to polyvinylidine difluoride (PVDF) membranes (Millipore Corporation, USA). The blot was blocked in blocking buffer (5% non-fat dry milk in TBST) for 2 h at room temperature, and then incubated with a dilute solution (1 : 500–1 : 1000) of caspase-3, Bax or bcl-2 antibodies (BioLegend, USA) in blocking buffer overnight at 4 °C. The blot was then incubated with an appropriate secondary antibody (ZSGB-BIO, Beijing, China) (1 : 5000–1 : 10 000 dilution), and β-actin (ZSGB-BIO, Beijing, China) was used as a loading control. The protein bands were visualized using the Gel Imaging System (ChemDoc-It610, UVP, USA).

## Conflicts of interest

The authors confirm that this article content has no conflicts of interest.

## Acknowledgements

This work was financially supported by the National Natural Science Foundations of China (no. 21171079) and the Recruitment Program of Global Experts (1000 Talents Plan).

## References

1 Z. Chen, *et al.*, Low-dose carbon monoxide inhalation protects neuronal cells from apoptosis after optic nerve crush, *Biochem. Biophys. Res. Commun.*, 2016, **469**(4), 809–815.
2 D. E. Stec, H. A. Drummond and T. Vera, Role of carbon monoxide in blood pressure regulation, *Hypertension*, 2008, **51**(3), 597–604.
3 L. E. Otterbein, *et al.*, Carbon monoxide has anti-inflammatory effects involving the mitogen-activated protein kinase pathway, *Nat. Med.*, 2000, **6**(4), 422.
4 S. W. Ryter and A. M. Choi, Targeting heme oxygenase-1 and carbon monoxide for therapeutic modulation of inflammation, *Transl. Res.*, 2016, **167**(1), 7–34.
5 L. E. Otterbein, Carbon monoxide: innovative anti-inflammatory properties of an age-old gas molecule, *Antioxid. Redox Signaling*, 2002, **4**(2), 309–319.
6 C. A. Piantadosi, Carbon monoxide, reactive oxygen signaling, and oxidative stress, *Free Radicals Biol. Med.*, 2008, **45**(5), 562–569.

7 M. A. Rhodes, *et al.*, Carbon monoxide, skeletal muscle oxidative stress, and mitochondrial biogenesis in humans, *Am. J. Physiol.*, 2009, **297**(1), H392–H399.
8 B. Wegiel, B. Y. Chin and L. E. Otterbein, Inhale to survive, cycle or die? Carbon monoxide and cellular proliferation, *Cell Cycle*, 2008, **7**(10), 1379–1384.
9 A. S. Almeida, *et al.*, Carbon monoxide modulates apoptosis by reinforcing oxidative metabolism in astrocytes role of Bcl-2, *J. Biol. Chem.*, 2012, **287**(14), 10761–10770.
10 S. Brouard, *et al.*, Carbon monoxide generated by heme oxygenase 1 suppresses endothelial cell apoptosis, *J. Exp. Med.*, 2000, **192**(7), 1015–1026.
11 T. R. Johnson, *et al.*, Metal carbonyls: a new class of pharmaceuticals?, *Angew. Chem., Int. Ed.*, 2003, **42**(32), 3722–3729.
12 R. Motterlini and L. E. Otterbein, The therapeutic potential of carbon monoxide, *Nat. Rev. Drug Discovery*, 2010, **9**(9), 728.
13 S. Romanski, *et al.*, Iron dienylphosphate tricarbonyl complexes as water-soluble enzyme-triggered CO-releasing molecules (ET-CORMs), *Organometallics*, 2012, **31**(16), 5800–5809.
14 R. Motterlini, *et al.*, Carbon monoxide-releasing molecules: characterization of biochemical and vascular activities, *Circ. Res.*, 2002, **90**(2), e17–e24.
15 A. J. Atkin, *et al.*, Modification of the deoxy-myoglobin/carbonmonoxy-myoglobin UV-vis assay for reliable determination of CO-release rates from organometallic carbonyl complexes, *Dalton Trans.*, 2011, **40**(21), 5755–5761.
16 I. Ott, *et al.*, Antitumor-active cobalt– alkyne complexes derived from acetylsalicylic acid: studies on the mode of drug action, *J. Med. Chem.*, 2005, **48**(2), 622–629.
17 S. D. Schimler, D. J. Hall and S. L. Debbert, Anticancer (hexacarbonyldicobalt) propargyl aryl ethers: Synthesis, antiproliferative activity, apoptosis induction, and effect on cellular oxidative stress, *J. Inorg. Biochem.*, 2013, **119**, 28–37.
18 S. Top, A. Vessières and G. Jaouen, Synthetic strategy for organometallic complexes of rhenium with exceptionally high affinity for the oestradiol receptor; their potential use as imaging and therapeutic agents, *J. Chem. Soc., Chem. Commun.*, 1994, **4**, 453–454.
19 P. Sawle, *et al.*, Carbon monoxide-releasing molecules (CO-RMs) attenuate the inflammatory response elicited by lipopolysaccharide in RAW264, 7 murine macrophages, *Br. J. Pharmacol.*, 2005, **145**(6), 800–810.
20 W.-Y. Lee, *et al.*, The induction of heme oxygenase-1 suppresses heat shock protein 90 and the proliferation of human breast cancer cells through its byproduct carbon monoxide, *Toxicol. Appl. Pharmacol.*, 2014, **274**(1), 55–62.
21 Y. Gong, *et al.*, Synthesis, toxicities and cell proliferation inhibition of CO-releasing molecules containing cobalt, *Transition Met. Chem.*, 2015, **40**(4), 413–426.
22 T. Tsubomura, *et al.*, Highly active antitumor platinum(II) complexes of amino sugars, *Inorg. Chem.*, 1990, **29**(14), 2622–2626.
23 N. D. Sachinvala, *et al.*, Synthesis, characterization, and anticancer activities of the first platinum complexes from sucrose, *J. Med. Chem.*, 1993, **36**(12), 1791–1795.
24 Y. Chen, *et al.*, A carbohydrate-linked cisplatin analogue having antitumor activity, *Angew. Chem., Int. Ed.*, 1999, **38**(12), 1768–1769.
25 Y. Mikata, *et al.*, Unprecedented sugar-dependent in vivo antitumor activity of carbohydrate-pendant cis-diammine-dichloroplatinum(II) complexes, *Bioorg. Med. Chem. Lett.*, 2001, **11**(23), 3045–3047.
26 I. Brudziñska, *et al.*, Synthesis, structural characterization, and antitumor activity of palladium(II) complexes containing a sugar unit, *Bioorg. Med. Chem. Lett.*, 2004, **14**(10), 2533–2536.
27 D. Schlawe, *et al.*, Iron-Containing Nucleoside Analogues with Pronounced Apoptosis-Inducing Activity, *Angew. Chem., Int. Ed.*, 2004, **43**(13), 1731–1734.
28 B. Levi and M. J. Werman, Fructose and related phosphate derivatives impose DNA damage and apoptosis in L5178Y mouse lymphoma cells, *J. Nutr. Biochem.*, 2003, **14**(1), 49–60.
29 K. Schmidt, *et al.*, Acetylenehexacarbonyldicobalt complexes, a novel class of antitumor drugs, *Inorg. Chim. Acta*, 2000, **306**(1), 6–16.
30 T. Roth, *et al.*, Comparative action of cobalt carbonyl complexes on cancer cells using human tumor xenografts, *Anticancer Res.*, 2002, **22**(4), 2281–2284.
31 S. Mandal and U. J. Nilsson, Tri-isopropylsilyl thioglycosides as masked glycosyl thiol nucleophiles for the synthesis of S-linked glycosides and glyco-conjugates, *Org. Biomol. Chem.*, 2014, **12**(27), 4816–4819.
32 M. Singer, *et al.*, Inhibition of carbonic anhydrase isozymes with benzene sulfonamides incorporating thio, sulfinyl and sulfonyl glycoside moieties, *Bioorg. Med. Chem. Lett.*, 2009, **19**(8), 2273–2276.
33 J. C. Morris, *et al.*, Targeting hypoxic tumor cell viability with carbohydrate-based carbonic anhydrase IX and XII inhibitors, *J. Med. Chem.*, 2011, **54**(19), 6905–6918.
34 F. M. Ibatullin, *et al.*, Reaction of 1, 2-trans-glycosyl acetates with thiourea: a new entry to 1-thiosugars, *Tetrahedron Lett.*, 2003, **44**(43), 7961–7964.
35 M. H. Jeon, *et al.*, A palladium and gold catalytic system enables direct access to O-and S-linked non-natural glycoconjugates, *Org. Biomol. Chem.*, 2016, **14**(48), 11518–11524.
36 S. I. van Kasteren, *et al.*, Expanding the diversity of chemical protein modification allows post-translational mimicry, *Nature*, 2007, **446**(7139), 1105.
37 M. F. Ebbesen, *et al.*, Cu elimination from Cu-coordinating macromolecules, *ACS Macro Lett.*, 2017, **6**(4), 399–403.
38 R. Šardzík, *et al.*, Preparation of aminoethyl glycosides for glycoconjugation, *Beilstein J. Org. Chem.*, 2010, **6**, 699.
39 Y. Gong, *et al.*, Toxicity, bio-distribution and metabolism of CO-releasing molecules based on cobalt, *Free Radicals Biol. Med.*, 2016, **97**, 362–374.
40 J. Li, *et al.*, Synthesis and biological activities of carbonyl cobalt CORMs with selectively inhibiting cyclooxygenase-2, *J. Organomet. Chem.*, 2018, **874**, 49–62.
41 P. Wang, *et al.*, Syntheses and evaluation of drug-like properties of CO-releasing molecules containing ruthenium and group 6 metal, *Eur. J. Med. Chem.*, 2014, **74**, 199–215.

 

42 P. V. Simpson, *et al.*, Synthesis, Cellular Uptake and Biological Activity Against Pathogenic Microorganisms and Cancer Cells of Rhodium and Iridium N-Heterocyclic Carbene Complexes Bearing Charged Substituents, *Eur. J. Inorg. Chem.*, 2013, **2013**(32), 5547–5554.

43 H. E. Jesse, *et al.*, Cytochrome bd-I in Escherichia coli is less sensitive than cytochromes bd-II or bo′′to inhibition by the carbon monoxide-releasing molecule, CORM-3: N-acetylcysteine reduces CO-RM uptake and inhibition of respiration, *Biochim. Biophys. Acta, Proteins Proteomics*, 2013, **1834**(9), 1693–1703.

44 K. Fujita, *et al.*, A Photoactive Carbon-Monoxide-Releasing Protein Cage for Dose-Regulated Delivery in Living Cells, *Angew. Chem., Int. Ed.*, 2016, **55**(3), 1056–1060.

45 K. Fujita, *et al.*, Intracellular CO release from composite of ferritin and ruthenium carbonyl complexes, *J. Am. Chem. Soc.*, 2014, **136**(48), 16902–16908.